

Cite this: *RSC Adv.*, 2015, 5, 33239

Aryl tosylates as non-ionic photoacid generators (PAGs): photochemistry and applications in cationic photopolymerizations†

 Edoardo Torti,^a Gioia Della Giustina,^b Stefano Protti,^{*a} Daniele Merli,^c
 Giovanna Brusatin^b and Maurizio Fagnoni^{*a}

The irradiation of various substituted aryl tosylates was investigated in a solution and homolysis of the ArO–SO₂C₆H₄CH₃ bond was the path exclusively observed. The corresponding phenols and photo-Fries adducts were obtained and *p*-toluenesulfinic and *p*-toluenesulfonic acids were liberated. The nature and amount of the acid photoreleased were tuned by changing the reaction conditions and the nature and position of the aromatic substituents. In deaerated solutions *p*-toluenesulfinic acid was formed exclusively, whereas under oxygenated conditions the stronger *p*-toluenesulfonic acid was released, as shown by HPLC ion chromatography analyses. ArO–S bond photocleavage takes place from the singlet state, as confirmed by laser flash photolysis experiments, and competitive intersystem crossing can make the aryl tosylate unreactive when a nitro group is present. The application of these aryl tosylates as non-ionic photoacid generators (PAGs) in hybrid organic/inorganic sol–gel photoresists has been explored.

Received 26th February 2015

Accepted 17th March 2015

DOI: 10.1039/c5ra03522h

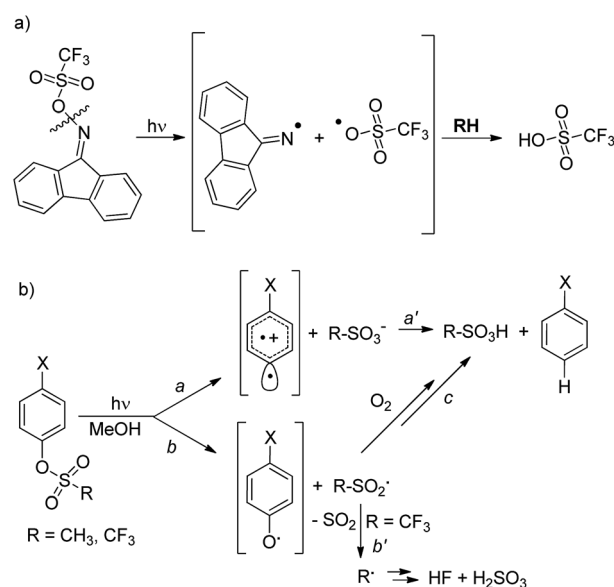
www.rsc.org/advances

Introduction

The development of new compounds able to release acid upon light absorption (so-called photoacid generators, PAGs) is of crucial importance in the field of materials chemistry and in microelectronics, photonics, nanofabrications and sensors development.¹ Aromatic onium salts (either iodonium or sulfonium) are widely used for this purpose as suitable “caged protons”.² Despite the thermal stability of the latter compounds, their poor solubility in polymer matrices³ has led to an increasing demand for more soluble non-ionic PAGs for photo(nano)lithography applications. The compounds proposed for this role usually release a sulfonic acid upon photocleavage of a weak N–O bond in iminosulfonates,^{4,5} imidosulfonates⁵ (Scheme 1a) or related compounds.⁶ Such cleavage generates a RSO₃• radical, which upon reaction with the medium, is able to form a strong sulfonic acid.

We recently reported, however, that sulfonic acids can be generated just as efficiently (>90%) by the irradiation of aryl mesylates and triflates, as shown in Scheme 1b. In this case,

two mechanisms compete, namely, heterolysis of the Ar–OS bond (path a) and homolysis of the ArO–S bond (path b), depending on the substituent X present on the aromatic ring and on the sulfonic moiety.^{7,8} In the former case, a sulfonic acid is released directly (path a'), whereas in the latter case trapping of the generated RSO₂• radical by oxygen leads to the formation



Scheme 1 (a) Photorelease of sulfonic acid upon the photocleavage of a N–O bond according to ref. 5c. (b) Competitive pathways in the photorelease of acids from (substituted) phenyl mesylates and triflates.

^aPhotogreen Lab, Department of Chemistry, University of Pavia, V. Le Taramelli 12, 27100 Pavia, Italy. E-mail: fagnoni@unipv.it; prottistefano@gmail.com; Fax: +39 0382 987323; Tel: +39 0382 987198

^bDepartment of Industrial Engineering, University of Padova and INSTM, Via Marzolo 9, 35131 Padova, Italy

^cDepartment of Chemistry, University of Pavia, V. Le Taramelli 12, 27100 Pavia, Italy

† Electronic supplementary information (ESI) available: Experimental procedures, copies of ¹H and ¹³C NMR spectra of compounds 1a–g, 3a–c, 3g, potentiometric titration of photolysed solutions of 1a–g in methanol. See DOI: 10.1039/c5ra03522h



of RSO_3H (path c) provided that fragmentation of the sulfonyl radical intermediate is avoided. Fragmentation occurs with aryl triflates, with the liberation of weak acids, such as HF and H_2SO_3 , in N_2 -equilibrated methanol (path b', Scheme 1b), rather than sulfonic acids.⁷

Release of strong acids thus does not depend on initial homolytic or heterolytic cleavage, and other aryl sulfonates appeared to be worth evaluating as photoacid generators. Aryl tosylates constitute a worthwhile target, because they are crystalline compounds, readily prepared from inexpensive reagents and more stable toward hydrolysis than other commonly used sulfonates (e.g. triflates). In addition, aryl tosylates have exhibited higher thermal stability than the corresponding mesylates when heated in a poly(4-hydroxystyrene) matrix.⁹ In fact, nitrobenzyl tosylates^{10,11} and *N*-oxysuccinimidoarylsulfonates¹² have previously been used for the photogeneration of *p*-toluenesulfonic acid (PTSA) and some iminotolates are commercially available for such an application (e.g. the iminotolate Irgacure PAG 121).

The photochemistry of aryl tosylates, however, has rarely been investigated¹³ and, to the best of our knowledge, the use of aryl tosylates as PAGs has only been tested with *o*-arenesulfonyloxanilide derivatives, where photorelease of PTSA was found to be almost quantitative, albeit with very low efficiency (Φ_{-1} ca. 0.05^{13b}).

The aim of this work is exploration of the photochemistry of some substituted phenyl tosylates, with an investigation of their product distribution in solution, as well as a test of their use as photoinitiators for acid-induced polymerization in innovative epoxy-based hybrid organic–inorganic systems obtained *via* sol-gel processes.¹⁴ These systems exhibit several attractive properties such as mechanical robustness, high thermal and chemical stability and transparency, and have found increasing interest within the field of photo(nano)lithography.¹⁵ Their preparation proceeds by hydrolysis and condensation reactions of organically modified alkoxides with formulas $\text{R}_n\text{Si}(\text{OR}')_{4-n}$ with the addition of an acidic or basic catalyst. The presence of a non-hydrolyzable Si–C bond provides a stable linkage between the organic unit and the oxide matrix, resulting in an inorganic three-dimensional network with pendant moieties that can be derivatized (e.g. double bonds or, as in our case, acid-sensitive epoxy rings) and lead to crosslinking.

Results

We have examined a series of phenyl sulfonates substituted with both electron-donating and electron-withdrawing groups

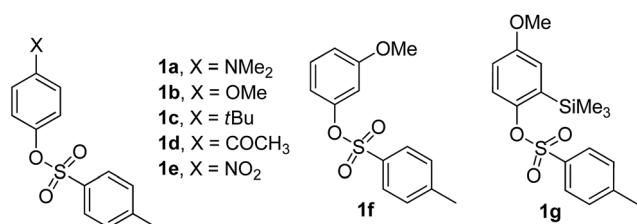


Chart 1

(**1a–f** in Chart 1). The silylated derivative **1g** was also tested because we previously demonstrated that the presence of silicon-based substituents was able to influence the photo-reactivity of aryl sulfonates.^{16,17} These were synthesized from the corresponding phenols.¹⁸

The photophysical and photochemical properties of tosylates **1a–g** are presented in Table S1 and Fig. S1–S7 (see ESI†). Two absorption maxima in the UV region around 260–290 nm ($\epsilon > 5000 \text{ L cm}^{-1} \text{ mol}^{-1}$) and 220–240 nm ($\epsilon > 10^4 \text{ L cm}^{-1} \text{ mol}^{-1}$) were observed for compounds **1a–c** and **1e–g**, whereas compound **1d** exhibited a single significant absorption at 239 nm ($\epsilon = 17\,800 \text{ L cm}^{-1} \text{ mol}^{-1}$). All the tosylates investigated exhibited low (**1a,b**: $\Phi_{\text{F}} < 0.01$) or negligible (**1c–g**) fluorescence emission (Table S1†).

The photochemistry of 4-methoxyaryl tosylate **1b** was investigated initially (Table 1) and its disappearance quantum yield (Φ_{-1}) was measured. This turned out to be modest in all the solvents tested ($\Phi_{-1} = 0.07\text{--}0.14$). Photolysis of **1b** under UV irradiation ($\lambda = 254 \text{ nm}$) caused ArO–S bond cleavage exclusively and 4-methoxyphenol **2b** and *o*-tosylphenol **3b** (a photo-Fries adduct) were formed in variable amounts depending on the solvent employed. Compound **3b** was the predominant product formed in cyclohexane, whereas the amount of **2b** increased with solvent proticity (methanol, 2-methoxyethanol) or in the presence of labile C–H bonds (e.g. in the case of THF, see Tables 1 and S2†). No products arising from Ar–OS bond cleavage, such as anisole or 1,4-dimethoxybenzene, were detected, in contrast to what was observed for other methoxy-aryl sulfonates.⁷ Irradiation in neat acetone (a triplet sensitizer)

Table 1 Irradiation of aryl tosylate **1b** in neat solvents^a

Solvent	Φ_{-1}	2b (%)	3b (%)
Cyclohexane	—	4	68
CH_2Cl_2	0.08 ^b	12	33
$\text{CH}_3\text{COOCH}_2\text{CH}_3$	—	26	36
THF	—	39	24
CH_3COCH_3	—	30	10
CH_3CN	0.13 ^b	24	30
$\text{CH}_3\text{OCH}_2\text{CH}_2\text{OH}$	0.07 ^b	34	29
CH_3OH	0.14 ^b	41	28

^a A nitrogen-saturated solution of **1b** (10^{-2} M) in the chosen solvent irradiated at 254 nm ($4 \times 15 \text{ W Hg lamps}$, 2 h) until $>80\%$ consumption of **1b** was achieved. Product yields calculated on the basis of the amount of **1b** consumed. ^b Disappearance quantum yield (Φ_{-1}) measured for a 10^{-2} M **1b** solution in the chosen solvent ($\lambda = 254 \text{ nm}$, $1 \times 15 \text{ W Hg lamp}$) using potassium ferrioxalate as actinometer.



likewise caused complete consumption of **1b**, giving **2b** as the main product. The same experiment carried out in oxygenated acetone led to no **1b** consumption.

The photolyzed solution in methanol was subjected to potentiometric titration and ionic chromatography analyses, revealing that 4-tolylsulfonic acid was liberated in modest yield (*ca.* 40%, Fig. S10, ESI†).

With these results in hand, we proceeded to investigate the photorelease of sulfinic and sulfonic acids from tosylates **1a–g** in methanol under both nitrogen- and oxygen-saturated conditions (Tables 2 and 3, Fig. S8–S19†). Under deaerated conditions, the Φ_{-1} measured was in the 0.1–0.15 range except for **1d**, in which the MeCO-group provides higher photo-reactivity ($\Phi_{-1} = 0.29$), and **1e** which is virtually photostable under these conditions (Table 2). It is notable that the presence of a trimethylsilyl group makes the tosylate more photoreactive (compare the Φ_{-1} value of **1b** with **1g**, Table 2).

Cleavage of the sulfonyl group upon UV light absorption led either to phenols **2** or to photo-Fries adducts **3**, in analogy with what had previously been observed for **1b**. Formation of **3** was exclusive when a strong electron-donating group (FG = NMe₂) was present, negligible with electron-withdrawing groups (*e.g.* MeCO, Table 2) or of the same magnitude as **2** with less strongly donating groups (FG = OMe, *t*Bu). Photocleavage of the ArO–S bond occurred independently of the nature and position of the substituents present on the aromatic ring (except for the case of unreactive **1e**). Formation of photo-Fries products, on the contrary, depended on the position, as shown by the different

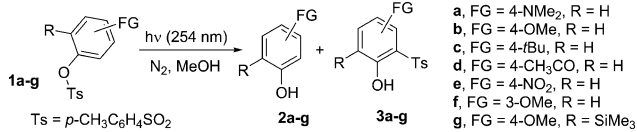
Table 3 Amount and type of acid released upon the irradiation of **1a–g** in oxygen-saturated methanol^a

ArOTs	H ⁺ ^b (% yield)	Anions ^c (% yield)
1a	46	CH ₃ C ₆ H ₄ SO ₃ H (53)
1b	82	CH ₃ C ₆ H ₄ SO ₃ H (82) ^d
1c	96	CH ₃ C ₆ H ₄ SO ₃ H (90)
1d	100	CH ₃ C ₆ H ₄ SO ₃ H (100)
1e	^e	^e
1f	99	CH ₃ C ₆ H ₄ SO ₃ H (95)
1g	84	CH ₃ C ₆ H ₄ SO ₃ H (77)

^a A 10^{−2} M solution of tosylates **1a–g** in oxygen-saturated methanol irradiated for 2 h at 254 nm (4 × 15 W Hg lamps). ^b Determined by potentiometric titration. ^c Determined by means of HPLC ion chromatography analyses. ^d CH₃C₆H₄SO₂H (<4%) was likewise formed. ^e No consumption of **1e** was observed.

results for isomeric **1b** and **1f** (no Fries adduct in the latter case). In some cases, the reaction was very clean as demonstrated by the UV-monitored conversion of **1d** to *p*-acetylphenol **2d** (see Fig. S20 and S21†). With respect to the release of acid, *p*-toluenesulfonic acid was formed in variable amounts in nitrogen-saturated methanol, with the single exception of tosylate **1d**, for which a mixture of sulfinic acid and PTSA was observed. As expected, the higher the amount of phenol **3** formed, the smaller was the amount of acid released (Table 2). Notably, the disappearance quantum yield (Φ_{-1}) values for **1b** and **1d** were not affected by the presence of oxygen (Table 2).

Table 2 Irradiation experiments on aryl tosylates **1a–g** in neat nitrogen-purged methanol

					
1	λ_{\max}^a (nm), ϵ /(L mol ^{−1} cm ^{−1})	Φ_{-1}^b	Photoproduct ^c , (%)	H ⁺ ^d (%)	Acids ^e (% yield)
1a	231, 8241 264, 10 287 317, 1171	0.11	3a , 100	^f	^f
1b	227, 21 190 274, 2423	0.14 ^g	2b , 41 3b , 28	40	CH ₃ C ₆ H ₄ SO ₂ H, 38 CH ₃ C ₆ H ₄ SO ₃ H, < 1 ^h
1c	227, 15 060 263, 1230	0.14	2c , 52 3c , 18	50	CH ₃ C ₆ H ₄ SO ₂ H, 48
1d	232, 28 320	0.29 ^g	2d , 73	67	CH ₃ C ₆ H ₄ SO ₂ H, 45 ^h CH ₃ C ₆ H ₄ SO ₃ H, 29
1e	227, 7980 264, 6350	<0.01	ⁱ	^f	^f
1f	224, 20 940 273, 3057	0.11	2f , 52	49	CH ₃ C ₆ H ₄ SO ₂ H, 47
1g	228, 17 100 285, 2010	0.21	2g , 21 3g , 18	32	CH ₃ C ₆ H ₄ SO ₂ H, 22 ^h

^a Maximum absorption wavelength and molar absorption coefficient. ^b Disappearance quantum yield measured for a 10^{−2} M **1a–g** solution in MeOH ($\lambda = 254$ nm, 1 × 15 W Hg lamp) using potassium ferrioxalate as actinometer. ^c Isolated yields. 2 h irradiation time (complete consumption of **1a–g**). ^d Determined by potentiometric titration. ^e Determined by HPLC ion chromatography analyses. ^f No acid released. ^g A similar Φ_{-1} value was measured under oxygen-saturated conditions. ^h Formic acid (<1%) detected. ⁱ No photoproducts detected by GC analysis.



On the other hand, under oxygenated conditions, a large amount of PTSA was released depending on the tosylate used (up to quantitative yield for **1d**) and the corresponding sulfinic acid was found only as a minor product in the case of **1b**. The lowest yield of released PTSA was found in the photolysis of **1a** (Table 3).

Some mechanistic studies were carried out with tosylates **1b** and **1d** as well as the photostable **1e**. Laser flash photolysis at 266 nm of an argon-saturated solution of **1b** (*ca.* 10^{-4} M) in methanol revealed the rapid formation (within a few ns) of two intense absorption bands with $\lambda_{\text{max}} = 330$ nm and 410 nm, respectively, with a weaker, broad absorption located at longer wavelengths (580–700 nm, Fig. 1a). The time evolution of these absorption bands indicated the presence of different transient species, with the predominant contribution from a long-lived intermediate ($\tau = 24$ μs , $k = 1.5 \times 10^{10} \text{ M}^{-1} \text{ s}^{-1}$) in both bands (see also Fig. S10†). Kinetic analysis revealed the presence of a second short-lived ($\tau = 4.1$ μs) species absorbing at 330 nm.

Shifting to an oxygen-saturated solution resulted in a slight modification of the transient absorption profile, with quenching of that portion of the 330 nm absorption attributable to the short-lived species (see Fig. 1a and b), while the kinetics of the

remaining absorption bands remained almost unchanged (Fig. 1a). A residual absorption around 300–350 nm, along with the broad band at 580–700 nm, was observed 150 μs after the laser pulse (see Fig. S22†).

With acetyl derivative **1d** (*ca.* 10^{-4} M in methanol, see Fig. 2a–c), two absorption bands ($\lambda_{\text{max}} = 330$ nm and 410 nm), along with a broad signal (580–700 nm, Fig. 2a), were again detected under argon-saturated conditions. Kinetic analysis revealed the presence of three different transient species, for which the longest-lived ($\tau = 33$ μs) represented the main contributor to both maxima, whereas two short-lived bands were observed at 340 ($\tau = 2.9$ μs) and 420 nm ($\tau = 0.7$ μs), respectively.

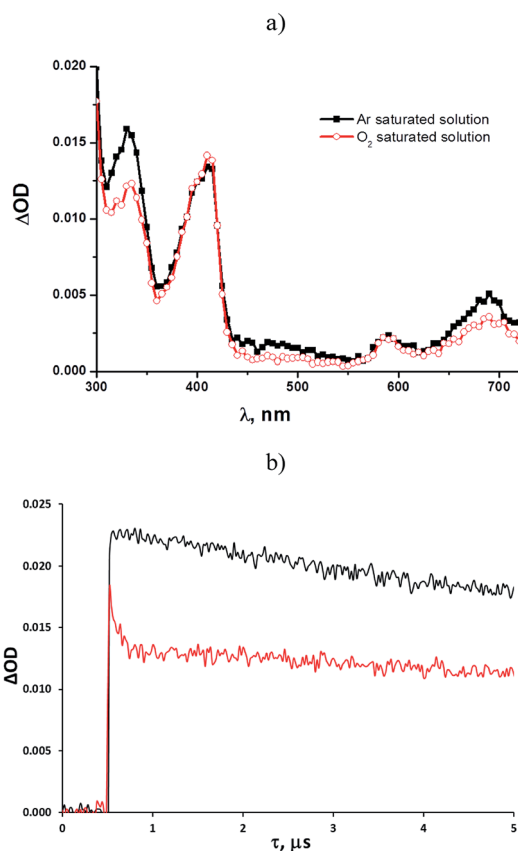


Fig. 1 Transient spectra of a solution of **1b** (10^{-4} M) in (a) argon-saturated methanol and O_2 -saturated methanol recorded 0.1 μs after a 20 ns laser pulse ($\lambda = 266$ nm); (b) profile of the absorbance change observed at 330 nm for a solution of **1b** in argon-saturated (black) and O_2 -saturated (red) methanol.

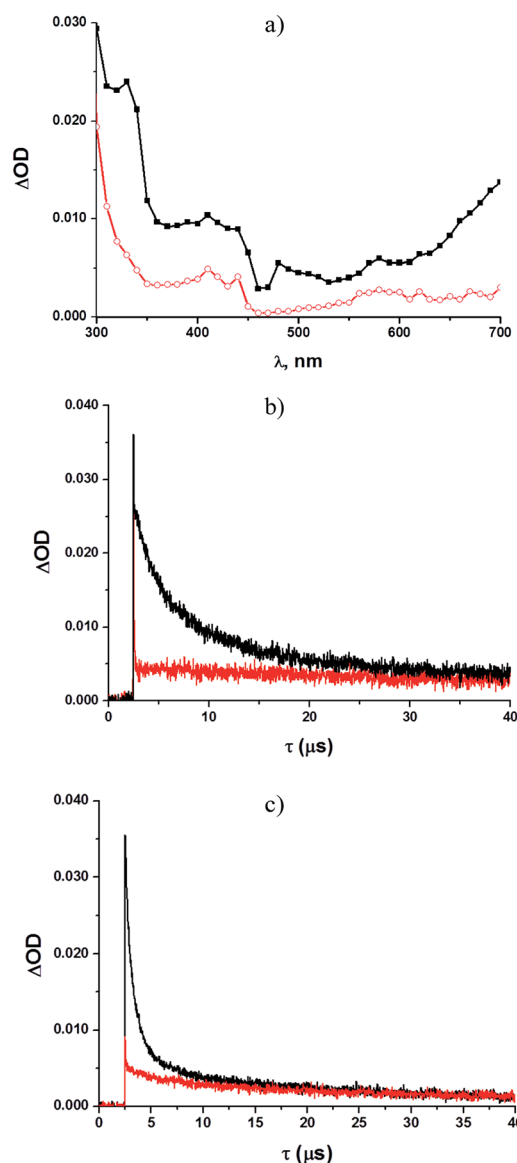


Fig. 2 Transient spectra of a solution of **1d** (10^{-4} M) in (a) argon-saturated methanol (black) and O_2 -saturated methanol (red) recorded 0.1 μs after a 20 ns laser pulse ($\lambda = 266$ nm); Profile of the absorbance change observed at (b) 340 nm and (c) 420 nm for a solution of **1d** in argon-saturated (black) and O_2 -saturated (red) methanol.



The latter was the main contributor to the broad absorption band at 580–700 nm. Shifting to an oxygen-saturated solution resulted in the quenching of the two short-lived intermediates (see Fig. 2b and c), whereas no significant effects were observed for the longest-lived species. In contrast, no significant transient species were observed with the nitro derivative **1e**.

The results obtained in solution encouraged us to determine the efficiency of the photoactive aryl tosylates **1a–d** and **1f–g** in photoinduced cationic polymerization processes. With this aim, their inclusion in a hybrid organic–inorganic photoresist (G8Ge2), obtained *via* acid-catalyzed condensation of 3-glycidyloxypropyltrimethoxysilane (GPTMS) and germanium tetraethoxide (TEOG) in 2-methoxyethanol, was planned.¹⁹ Preliminary experiments to determine the effect of the photoresist components were first carried out on **1d**, for which the generation of PTSA was most efficient in methanol. Irradiation of **1d** was carried out in oxygen-saturated 2-methoxyethanol and PTSA was photoreleased in 71% yield, analogous to what was found in neat oxygen-saturated methanol. The presence of GPTMS (0.73 M), germanium tetraethoxide (TEOG, 0.18 M) and H₂O (2.55 M) produced comparable results (PTSA yield = 57%).²⁰

At this point, tests were carried out on the assembled G8Ge2 containing acid-sensitive epoxy functionalities obtained *via* sol-gel techniques from GPTMS and TEOG (molar ratio: 80 : 20) in 2-methoxyethanol.²¹ The synthesized aryl tosylates were then incorporated in the G8Ge2 system and the resulting sol was spin-coated on silicon (100) substrates. The films obtained were then exposed to UV light (Hg–Xe UV spot light source) at increasing doses and the structural modifications induced by aryl tosylates were investigated by means of both UV and FT-IR analysis.

Fig. 3a illustrates the UV-vis spectra of the hybrid samples before and after addition of **1d** to the sample. An absorption band at 240 nm, due to the presence of aryl tosylate **1d** (1%), was apparent and was markedly reduced within the first minute of UV irradiation. Among the vibrational modes that characterize the epoxy moiety in G8Ge2, the signals assigned to C–H stretching at 3060 and 3000 cm^{−1} were chosen to determine the degree of polymerization (see Fig. 3b).¹⁹

As shown in Fig. 3b for the G8Ge2/**1d** system, UV irradiation caused a decrease in absorbance in the bands at 3060 and 3000 cm^{−1}, indicating gradual ring-opening of the epoxy moiety with subsequent formation of an interpenetrating organic network and densification of the exposed area. The degree of photopolymerization induced by phenyl tosylates **1a–d** and **1f–g** was then measured by monitoring the evolution of epoxy ring-opening as a function of the UV dose. The degree of polymerization (at least within the first three minutes of UV exposure, Fig. 3c) roughly followed the amount of PTSA photoreleased under oxygenated conditions (with **1d** the best and **1a** the worst of the series, see Table 3).

It is noteworthy that a degree of polymerization above 60% was achieved in all cases (except **1g**) after 18 min UV exposure. Photodegradation of the PAG (see Fig. 3a) was essentially complete in 1–2 min, while epoxy polymerization required

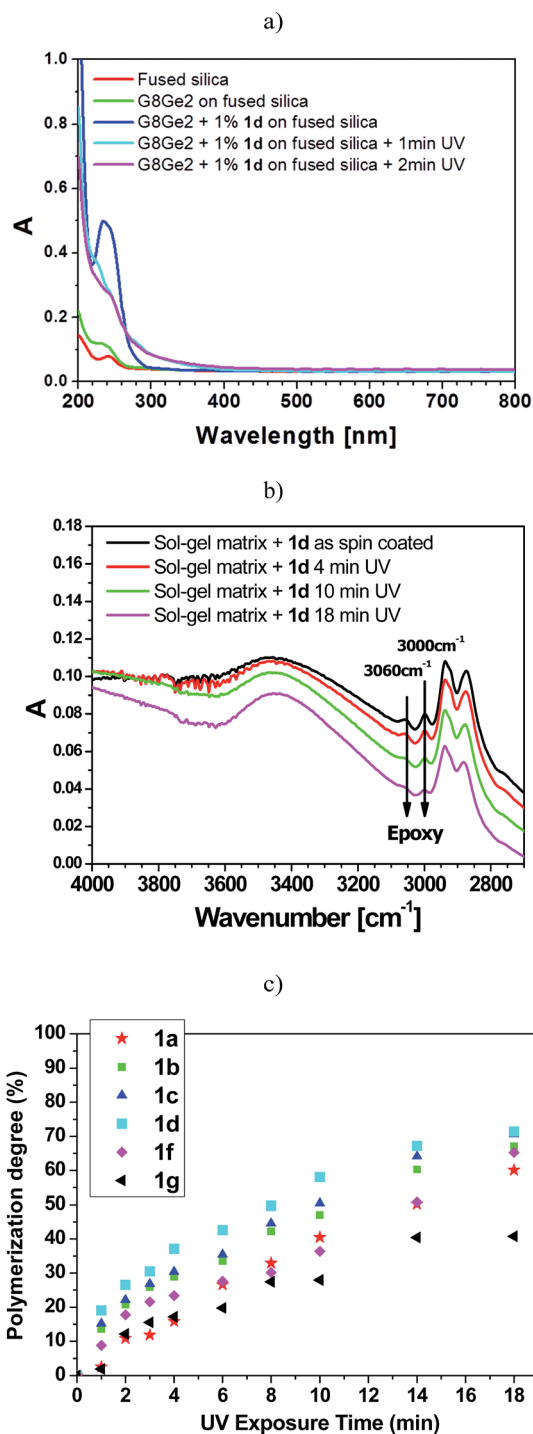


Fig. 3 (a) UV-vis spectra of the photoresist G8Ge2 in the 200–800 nm region in the absence and presence of 1% tosylate **1d** before and after UV irradiation; (b) FTIR spectra of G8Ge2 films in the 4000–2600 cm^{−1} region with 1% molar concentration of **1d** before and after UV irradiation. Samples were spin-coated on fused silica slides and silicon, respectively; and (c) degree of photopolymerization of epoxy groups *versus* UV curing time, achieved by 1% molar addition of aryl tosylates **1a–d**, **1f–g** to G8Ge2 sol-gel matrix.



several minutes (no polymerization took place when UV curing was carried out in the absence of **1a-g**).

Discussion

The photochemistry of phenyl 4-methylbenzenesulfonate was investigated in 1966 by Havinga *et al.*, who observed homolytic cleavage of the ArO–S bond.²² More recently, our research group noticed competition between ArO–S bond homolytic cleavage and Ar–OS heterolysis taking place in aryl triflates, mesylates,⁷ nonaflates²³ and imidazylates.²⁴ For the substrates examined in this paper, the homolytic pathway is exclusive, with subsequent formation of a phenoxy (**I**)/paratoluenesulfonyl (**II**) radical pair (see Scheme 2 below, path a).

Laser flash photolysis analyses of **1b** in methanol (Fig. 1a) showed two significant absorption bands at 330 and 410 nm. The oxygen-sensitive signal dominating at 330 nm was recognized as due to the 4-methylbenzenesulfonyl radical **II**, as previously suggested,^{12,25} whereas the long-lived intermediate with a maximum at 410 nm (and the portion of the 330 nm absorption not quenched by oxygen) can be confidently attributed to the 4-methoxyphenoxy radical **Ib**.²⁶ In the case of **1d**, however, LFP revealed the presence of an additional transient signal, assigned to triplet ³**1d** (absorption at 420 and 580–700 nm), accompanying the two radicals absorbing at 330 and 410 nm.

Photo-Fries reactions are known to arise mainly from excited singlets, although triplets have occasionally been suggested.²⁷ Our data show that cleavage of the ArO–S bond in the excited singlet is the pathway exclusively observed upon direct irradiation. A triplet is not involved, as confirmed by the lack of oxygen quenching of photocleavage for **1b** and **1d** (Table 2) and as further supported by LFP experiments. As for compound **1d**, none of the photoreactivity normally observed in triplet aromatic ketones (*e.g.* hydrogen abstraction) was found, even in an excellent hydrogen-donating solvent such as methanol. Triplets play a role only when cleavage from singlets does not take place, as in the case of **1e** where efficient intersystem crossing leads to a very short-lived triplet (lifetime in the $\tau =$

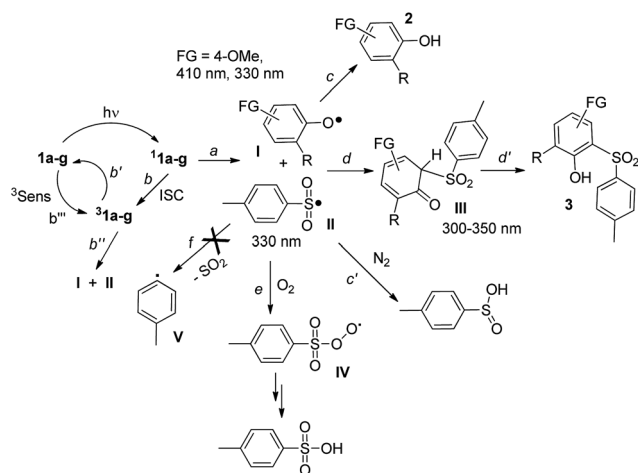
350–900 ps range in EtOH²⁸), thus preventing any photo-Fries reaction, in analogy with other nitroaryl esters (Scheme 2, paths b and b').²⁹ On the other hand, acetone-sensitized experiments on **1b** revealed that in some cases, when triplets were populated by sensitization, a photo-Fries reaction also took place (paths b''', b''), but was completely inhibited in oxygen-saturated solution.

Finally, in contrast to what was reported for other aryl sulfonates such as mesylates and triflates, heterolysis of the Ar–OS bond^{7,8,13a,16} plays no role in the photochemical behavior of these substrates, even in the presence of acetone as a triplet sensitizer.

When generated in N₂-saturated methanol, the resulting phenoxy and sulfonyl radical intermediates can follow two competing pathways. The first is escape from the solvent cage followed by hydrogen abstraction from the medium to give phenol **2** and paratoluenesulfinic acid, respectively (paths c and c'). On the other hand, direct recombination of the two radicals results in formation of the Fries rearrangement product **3**, *via* the cyclohexadienone intermediate **III** (paths d and d'). In the case of **1b**, the residual, persistent absorption at 300–350 nm and 600–700 nm (see Fig. S22 in ESI† and Fig. 1a) found in LFP experiments could be assigned to **III**, in analogy with what has already been reported about the photo-Fries rearrangement of naphthyl^{30a} and phenyl acetates.^{30b,c}

With the single exception of the nitroaryl tosylate **1e**, all the sulfonates examined displayed comparable photoreactivity in solution ($\Phi_{-1} = 0.11$ – 0.29 , the highest value measured for tosylate **1d**), but different product distributions. We reasoned that the stability of the phenoxy radical **I** and accordingly the O–H bond dissociation energy (BDE) of **2** could play a role in determining the fate of the reaction. As is apparent from Table 4, the lower the O–H BDE (*e.g.* 321.3 kJ mol^{−1} in the case of amino tosylate **1a**), the higher is the amount of the Fries adduct **3**, whereas formal hydrolysis to **2** is the sole reaction promoted for tosylates with electron-withdrawing substituents and stronger O–H bonds (*e.g.* BDE = 380.3 kJ mol^{−1} for **1d**).

Thus, competition between paths c, c' and d, d' (Scheme 2) depends on the nature and stability of the radical **I**. Recombination to **III** (paths d and d') is favored for electron-rich tosylates such as the amino derivative **1a**, making the photoinduced release of PTSA inaccessible. On the other hand, although the



Scheme 2 Photoreactivity of aryl tosylates **1a-g**.

Table 4 Comparison of the product distributions observed in the irradiation of tosylates **1a-f** in methanol with the O–H BDE values of phenols **2a-f**

O–H BDE for 2 (kJ mol ^{−1})	Ar–OTs	Photoproducts 2 : 3
321.3	1a	0 : 100
349.3	1b	60 : 40
364.3	1c	74 : 26
371.3	1f	100 : 0
380.3	1d	100 : 0
396.3	1e	— ^b
371.3	PhOTs	—

^a Measured values from ref. 31. ^b No significant consumption of **1e** observed.



presence of electron-withdrawing groups is desirable to maximize the yield of acid generated, moving to a stronger EWG (e.g. in the nitro derivative **1e**) completely inhibits the overall photoreactivity. A peculiar case is represented by **1g**. As previously observed in related sulfonate esters (mesylates, triflates),¹⁶ the presence of a silicon-based substituent ortho to the sulfonate moiety significantly increased the overall photoreactivity.¹⁶ The same behaviour was found here, although the cleavage shifted from heterolysis of an Ar–OS bond (in the cases of mesylate and triflate)¹⁶ to ArO–S homolysis (in the case of tosylate). The presence of oxygen promoted efficient trapping of the ArSO₂[•] radical **II** (Scheme 2, path e), prior to recombination with the phenoxy radical, and PTSA was obtained *via* the corresponding arylperoxysulfonyl radical **IV**.²⁵ Both experimental and spectroscopic data exclude SO₂ loss from **II** to afford the phenyl radical **V** (path f), in contrast to results previously reported for aryl sulfonyl radicals in acetonitrile.²⁵

Most of the aryl tosylates tested were found to be suitable PAGs for the release of PTSA to be used for cationic ring-opening of epoxy groups in sol–gel systems. When included in photoresists, compounds **1a–g** were the only species responsible for the absorption of light (see Fig. 3a). Acid release preceded polymerization (see the different rates observed for **1d** conversion and induced polymerization, see Fig. 3a and c), which is consistent with the key role of the substrates examined as PAGs. In this study, the efficiency of organic crosslinking of G8Ge2 acid-labile moieties depended on the tosylate used, the most favourable case being the acetyl derivative **1d**. Furthermore, in contrast to what was observed for other aryl sulfonates,⁷ where competing pathways affected the yield and quality of the generated acids, photodecomposition of aryl tosylates proceeds *via* an unambiguous mechanism, and strong PTSA was the only acid obtained during irradiation in oxygenated solutions.

Conclusion

Summing up, the photochemistry of substituted phenyl tosylates proceeds exclusively *via* ArO–S bond homolytic cleavage to generate a phenoxy/sulfonyl radical pair. Depending on the reaction conditions, either paratoluenesulfinic or paratoluenesulfonic acid can be released, the latter being obtained exclusively under oxygenated conditions. It can be noted that acids are photoreleased even in the solid state. The results highlight the potential of aryl tosylates as a promising class of non-ionic PAGs, able to promote cationic polymerization of epoxy groups in hybrid sol–gel photoresists. Furthermore, structural changes can result in a decrease in the solubility of exposed areas in organic or suitable solvents. This peculiarity can be exploited for photo(nano)lithography on sol–gel materials, which plays an important role in the realization of many devices.³²

Experimental

General information

NMR spectra were recorded on a 300 MHz spectrometer. Attributions were made on the basis of ¹H and ¹³C NMR, as well as DEPT-135 experiments; chemical shifts are reported in ppm

downfield from TMS. The photochemical reactions were performed using nitrogen- or oxygen-saturated solutions in quartz tubes in a multi-lamp reactor fitted with 4 × 15 W Hg lamps (emission centered at 254 nm) for irradiation. The reaction course was followed by GC analyses and the products formed were identified and quantified by comparison with authentic samples. Work-up of the photolyses involved concentration *in vacuo* and chromatographic separation using silica gel. Solvents of HPLC purity were employed in the photochemical reactions. Quantum yields were measured at 254 nm (1 Hg lamp, 15 W).

The acidity released was determined from 5 mL of the photolysed solutions by dilution with water (25 mL) and titration with aqueous 0.1 M NaOH by means of a potentiometer equipped with a pH glass combined electrode module. *para*-Toluenesulfonic (PTSA), *para*-toluenesulfinic and formic acid were determined *via* HPLC ion chromatography and quantified by means of a calibration curve obtained with commercially available samples.

Nano-to-microsecond transient absorption experiments were performed using a nanosecond laser flash photolysis apparatus equipped with a 20 Hz Nd:YAG laser (20 ns, 1 mJ at 266 nm) and a 150 W Xe flash lamp as the probe light. Samples were placed in a quartz cell (10 × 10 mm section) at a concentration adjusted to obtain an OD value of 1.0 at 266 nm.

Phenols **2b–f**, 3-glycidyloxypropyltrimethoxysilane (GPTMS) and germanium tetraethoxide (TEOG) were commercially available and used as received. 4-*N,N*-Dimethylaminophenol **2a**^{13a} and 4-methoxy-2-trimethylsilylphenol **2g**¹⁶ were prepared by known procedures.

Synthesis of aryl tosylates **1a–g**

Compounds **1a–g** were synthesized by adapting a known procedure.¹⁸ To a solution of the chosen phenol (20 mmol) in dichloromethane (80 mL) and triethylamine (15 mL) at room temperature, *p*-toluenesulfonyl chloride (24 mmol) was added portionwise and the resulting mixture was stirred overnight. Water (25 mL) was then added and the resulting mixture was stirred for an additional 3 h. The mixture was then extracted with ethyl acetate (4 × 50 mL) and the organic layers were reunited and washed with water (3 × 50 mL), 10% aqueous HCl (3 × 150 mL, except in the case of **1a**), water (2 × 150 mL), saturated aqueous NaHCO₃ (2 × 150 mL) and brine (2 × 100 mL), and dried over Na₂SO₄. The solvent was evaporated under vacuum. The resulting residue was purified by column chromatography or recrystallization.

4-*N,N*-Dimethylaminophenyl *p*-toluenesulfonate (1a**).** Obtained in 72% yield from 4-*N,N*-dimethylaminophenol (**2a**),^{13a} purification by column chromatography (eluant: cyclohexane/ethyl acetate 9/1). Colorless solid, mp = 123–125 °C, lit.^{13a} 117–120 °C. Spectroscopic data for **1a** are in accordance with the literature.¹⁸ Anal. calcd for C₁₅H₁₇NO₃S: C, 61.83; H, 5.88; N, 4.81. Found: C, 61.8; H, 5.9; N, 4.8.

4-Methoxyphenyl *p*-toluenesulfonate (1b**).** Obtained in 89% yield from 4-methoxyphenol **2b**. Purification by column chromatography (eluant: cyclohexane/ethyl acetate 9/1). Colorless solid, mp = 67–70 °C, lit.¹⁸ 69–70 °C. Spectroscopic data for **1b**



are in accordance with the literature.¹⁸ Anal. calcd for $C_{14}H_{14}O_4S$: C, 60.42; H, 5.07. Found: C, 60.4; H, 5.1.

4-tert-Butylphenyl p-toluenesulfonate (1c). Obtained in 85% yield from 4-tert-butylphenol (**2c**), colorless solid, mp = 112–114 °C (from MeOH/H₂O), lit.³³ 113–115 °C. Spectroscopic data for **1c** are in accordance with the literature.³³ Anal. calcd for $C_{17}H_{20}O_3S$: C, 67.08; H, 6.62. Found: C, 67.1; H, 6.6.

4-Acetylphenyl p-toluenesulfonate (1d). Obtained in 71% yield from 4-hydroxyacetophenone (**2d**). Colorless solid, mp = 71–73 °C (from MeOH/H₂O), lit.³⁴ 69–70 °C. Spectroscopic data for **1d** are in accordance with the literature.¹⁸ Anal. calcd for $C_{15}H_{14}O_4S$: C, 62.05; H, 4.86. Found: C, 62.0; H, 4.8.

4-Nitrophenyl p-toluenesulfonate (1e). Obtained in 62% yield from 4-nitrophenol (**2e**). Pale yellow solid, mp = 102–104 °C (from MeOH/H₂O), lit.³⁵ 98 °C. Spectroscopic data for **1e** are in accordance with the literature.³⁵ Anal. calcd for $C_{13}H_{11}NO_5S$: C, 53.24; H, 3.78; N, 4.78. Found: C, 53.2; H, 3.8; N, 4.9.

3-Methoxyphenyl p-toluenesulfonate (1f). Obtained in 68% yield from 3-methoxyphenol (**2f**). Colorless solid, mp = 49–51 °C (from MeOH/H₂O), lit.³⁶ 59–60 °C. Spectroscopic data are in accordance with the literature.³⁶ Anal. calcd for $C_{14}H_{14}O_4S$: C, 60.42; H, 5.07. Found: C, 60.6; H, 5.2.

4-Methoxy-2-trimethylsilylphenyl p-toluenesulfonate (1g). Obtained in 55% yield from 4-methoxy-2-trimethylsilylphenol (**2g**).¹⁶ Purification by column chromatography (eluant: cyclohexane/ethyl acetate 9 : 1). Colorless solid, mp = 60–62 °C. **1g**: ¹H NMR (CDCl₃, δ) 7.85–7.35 (AA'BB' system, 4H), 6.95 (m, 2H), 6.75 (dd, 1H, *J* = 3 Hz and 9 Hz), 3.80 (s, 3H), 2.45 (s, 3H), 0.30 (s, 9H). ¹³C NMR (CDCl₃, δ) 157.0, 148.4, 145.0, 134.2, 134.0, 129.7 (CH), 128.2 (CH), 121.0 (CH), 120.5 (CH), 114.5 (CH), 55.4 (CH₃), 21.6 (CH₃), –0.7 (CH₃). IR (neat, ν /cm^{–1}): 2956, 1467, 1370, 1194, 1179, 1157, 1093, 1037. Anal. calcd for $C_{17}H_{22}O_4SSi$: C, 58.25; H, 6.33. Found: C, 58.2; H, 6.2.

Preparative irradiations

Irradiation of 4-*N,N*-dimethylaminophenyl p-toluenesulfonate (1a) in MeOH. A nitrogen-saturated solution of **1a** (440 mg, 1.5 mmol, 0.03 M) in MeOH was irradiated for 4 h at 254 nm. The photolysed solution was then evaporated and the resulting residue was purified by column chromatography (eluant: cyclohexane/ethyl acetate 9 : 1) to afford 330 mg 4-*(N,N*-dimethylamino)-2-*(p*-toluenesulfonyl)phenol (**3a**, colorless solid, 75% yield, mp = 133–135 °C). **3a**: ¹H NMR (CDCl₃, δ): 8.55 (s, 1H), 7.80–7.30 (AA'BB' system, 4H), 6.90–6.80 (m, 3H), 2.80 (s, 6H), 2.40 (s, 3H). ¹³C NMR (CDCl₃, δ) 146.0, 145.0, 144.4, 138.9, 129.9 (CH), 126.7 (CH), 123.5, 121.8 (CH), 119.6 (CH), 110.9 (CH), 41.0 (CH₃), 21.5 (CH₃). IR (neat, ν /cm^{–1}): 3377, 2924, 1503, 1139, 1090, 963. Anal. calcd for $C_{15}H_{17}NO_3S$: C, 61.83; H, 5.88; N, 4.81. Found: C, 61.9; H, 6.1; N, 4.9.

Irradiation of 4-methoxyphenyl p-toluenesulfonate (1b) in MeOH. A nitrogen-saturated solution of **1b** (150 mg, 0.01 M) in MeOH (55 mL) was irradiated at 254 nm for 12 h (90% consumption of **1b**). The photolysed solution was then evaporated and the resulting residue was purified by column chromatography (eluant: cyclohexane/ethyl acetate 9 : 1) to give a mixture of 4-methoxy-2-*(p*-toluenesulfonyl)phenol (**3b**, 44 mg,

32% yield based on consumed **1b**) and unreacted **1b** (3 mg). **3b**: ¹H NMR (CDCl₃, from the mixture, δ) 7.85–7.30 (AA'BB', 4H), 7.15 (d, 1H, *J* = 3 Hz), 7.05 (dd, 1H, *J* = 3 and 9 Hz), 6.95 (d, 1H, *J* = 9 Hz), 6.80 (s, 1H), 3.70 (s, 3H), 2.40 (s, 3H). ¹³C NMR (CDCl₃, from the mixture) δ: 153.0, 149.7, 144.8, 138.4, 130.0 (CH), 126.8 (CH), 123.7 (CH), 123.4, 120.1 (CH), 111.2 (CH), 55.7 (CH₃), 21.5 (CH₃).

Irradiation of 4-tert-butylphenyl p-toluenesulfonate (1c) in MeOH. A nitrogen-saturated solution of **1c** (340 mg, 0.022 M) in methanol (50 mL) was irradiated for 6 h. The photolysed solution was then evaporated and the resulting residue was purified by column chromatography (eluant: cyclohexane/ethyl acetate 8 : 2) to afford 143 mg of a mixture of 4-tert-butylphenol (**2c**, 79 mg, 23%) and 4-tert-butyl-2-*(p*-toluenesulfonyl)phenol (**3c**, 64 mg, 19% yield). **3c**: ¹H NMR (from the mixture, CDCl₃) δ: 7.80–7.35 (AA'BB', 4H), 7.65 (d, 1H, *J* = 3 Hz), 7.48 (dd, 1H, *J* = 3 and 9 Hz), 7.35 (s, 1H), 6.90 (d, 1H, *J* = 9 Hz), 3.80 (s, 3H), 2.45 (s, 3H). ¹³C NMR (from the mixture, CDCl₃) δ: 153.4, 143.9, 138.4, 133.5 (CH), 130.0 (CH), 129.7, 126.7 (CH), 125.0 (CH), 123.4, 118.6 (CH), 34.2, 31.1 (CH₃). IR of the mixture (neat, ν /cm^{–1}): 3392, 2963, 1516, 1227, 1141, 831.

Irradiation of 4-methoxy-2-trimethylsilylphenyl p-toluenesulfonate (1g) in MeOH. A nitrogen-saturated solution of **1g** (180 mg, 0.01 M) in methanol (50 mL) was irradiated at 254 nm for 5 hours (90% consumption of **1g**). The photolysed solution was then evaporated and the resulting residue was purified by column chromatography (eluant: cyclohexane/ethyl acetate 9 : 1), to afford a mixture of 22 mg 4-methoxy-2-*(p*-toluenesulfonyl)-5-trimethylsilylphenol (**3g**, 14% yield based on consumed **1g**) along with 6 mg unreacted **1g**. **3g**: ¹H NMR (from the mixture, CDCl₃, δ) 9.05 (s, 1H), 7.85–7.30 (AA'BB', 4H), 7.15 (d, 1H, *J* = 3 Hz), 7.10 (d, 1H, *J* = 3 Hz), 3.80 (s, 3H), 2.40 (s, 3H), 0.30 (s, 9H). ¹³C NMR (from the mixture, CDCl₃, δ) 153.9, 152.6, 144.6, 136.4, 132.3, 129.9 (CH), 126.7 (CH), 126.4 (CH), 122.1, 111.6 (CH), 55.8 (CH₃), 21.5 (CH₃), –1.3 (CH₃).

Use of aryl tosylates 1a–g as PAGs in polymerization processes

The detailed protocol for the synthesis of the G8Ge2 system has already been described.²¹ As indicated above, GPTMS and TEOG are the main precursors of the sol and react in a molar ratio of 80 : 20 under acidic conditions to generate the G8Ge2 system with a final concentration of 150 (SiO₂ + GeO₂) g L^{–1}. Aryl tosylates **1a–d**, **1f–g** (1% mol with respect to the concentration of the starting material GPTMS) were incorporated in the sol. Films were deposited by spin-coating (spinning rate: 2000 rpm, spinning time: 30 s) on silicon (100) substrates and fused silica slides to give a thickness of about 1 μm.

The samples obtained were pre-baked for 30 min at 80 °C to remove residual solvent and irradiated with UV light for an increasing curing time using a Hg–Xe UV spot light source, enhanced in the UV region (254–365 nm range), with a power density of around 150 mW cm^{–2} on the sample surface. The progress of the photoinduced epoxy polymerization was followed by means of Fourier transform infrared spectroscopy (FT-IR) analyses. The analyses were performed in transmission mode within the 400–4000 cm^{–1} range with 4 cm^{–1} resolution



for a total of 32 scans. To evaluate and compare the efficiency of the different PAGs in the solid state, the epoxy polymerization degree for each PAG/sol-gel matrix system was assessed by collecting progressive FT-IR spectra with increasing UV exposure time (1–18 min); the area under the bands at 3000–3060 cm⁻¹, related to C–H stretching in the epoxy ring, was calculated by a Gaussian peak fitting procedure (Microcal Origin software).

Acknowledgements

S.P. acknowledges MIUR, Rome (FIRB-Futuro in Ricerca 2008 project RBFR08J78Q) for financial support and Prof. A. Albini (University of Pavia) and Prof. P. Hoggard (Santa Clara University) for fruitful discussions. This work has been supported by the Fondazione Cariplo (grant no. 2012-0186).

Notes and references

- 1 R. Ayothi, Y. Yi, H. B. Cao, W. Yueh, S. Putna and C. K. Ober, *Chem. Mater.*, 2007, **19**, 1434–1444; S.-Y. Moon and J.-M. Kim, *J. Photochem. Photobiol., C*, 2007, **8**, 157–173; M. Shirai and M. Tsunooka, *Bull. Chem. Soc. Jpn.*, 1998, **71**, 2483–2507; M. Shirai and M. Tsunooka, *Prog. Polym. Sci.*, 1996, **21**, 1–45; J. M. Frechét, *Pure Appl. Chem.*, 1992, **64**, 1239–1248.
- 2 J. V. Crivello, *J. Polym. Sci., Part A: Polym. Chem.*, 1999, **37**, 4241–4254.
- 3 K. L. Covert and D. J. Russell, *J. Appl. Polym. Sci.*, 1993, **49**, 657–671.
- 4 J. Lalevée, X. Allonas, J.-P. Fouassier, M. Shirai and M. Tsunooka, *Chem. Lett.*, 2003, **32**, 178–179.
- 5 (a) J. P. Malval, S. Suzuki, F. M. Savary, X. Allonas, J. P. Fouassier, S. Takahara and T. Yamaoka, *J. Phys. Chem. A*, 2008, **112**, 3879–3885; (b) M. Shirai, T. Yatsuo and M. Tsunooka, *J. Photopolym. Sci. Technol.*, 1996, **9**, 273–276; (c) M. Shirai and H. Okamura, *Prog. Org. Coat.*, 2009, **64**, 175–181; (d) L. Steidl, S. J. Jhaveri, R. Ayothi, J. Sha, J. D. McMullen, S. Y. C. Ng, W. R. Zipfel, R. Zentel and C. K. Ober, *J. Mater. Chem.*, 2009, **19**, 505–513.
- 6 M. Ikbali, R. Banerjee, S. Atta, A. Jana, D. Dhara, A. Anoop and N. D. P. Singh, *Chem.-Eur. J.*, 2012, **18**, 11968–11975 and references therein.
- 7 M. Terpolilli, D. Merli, S. Protti, V. Dichiarante, M. Fagnoni and A. Albini, *Photochem. Photobiol. Sci.*, 2011, **10**, 123–127.
- 8 D. Ravelli and M. Fagnoni, in *CRC Handbook of Organic Photochemistry and Photobiology*, ed. A. Griesbeck, M. Oelgemöeller and F. Ghatti, CRC Press, 3rd edn, 2012, pp. 393–417 and references therein.
- 9 G. G. Barclay, D. R. Medeiros and R. F. Sinta, *Chem. Mater.*, 1995, **7**, 1315–1324.
- 10 F. M. Houlihan, T. X. Neenan, E. Reichmanis, J. M. Kometani, L. F. Thompson, T. Chin and O. Nalamasu, *J. Photopolym. Sci. Technol.*, 1990, **3**, 259–273.
- 11 K. E. Uhrich, E. Reichmanis and F. A. Baiocchi, *Chem. Mater.*, 1994, **6**, 295–301; F. M. Houlihan, A. Shugard, R. Gooden and E. Reichmanis, *Macromolecules*, 1988, **21**, 2001–2006.
- 12 F. Ortica, C. Coenjarts, J. C. Scaiano, H. Liu, G. Pohlers and J. F. Cameron, *Chem. Mater.*, 2001, **13**, 2297–2304.
- 13 (a) M. De Carolis, S. Protti, M. Fagnoni and A. Albini, *Angew. Chem., Int. Ed.*, 2005, **44**, 1232–1236; (b) M. Ikbali, A. Jana, N. D. P. Singh, R. Banerjee and D. Dhara, *Tetrahedron*, 2011, **67**, 3733–3742.
- 14 L. L. Hench and J. K. West, *Chem. Rev.*, 1990, **90**, 33–72; C. Sanchez, B. Lebeau, F. Ribot and M. In, *J. Sol-Gel Sci. Technol.*, 2000, **19**, 31–38.
- 15 G. Brusatin and G. Della Giustina, *J. Sol-Gel Sci. Technol.*, 2011, **60**, 299–314.
- 16 E. Abitelli, S. Protti, M. Fagnoni and A. Albini, *J. Org. Chem.*, 2012, **77**, 3501–3507.
- 17 S. Crespi, D. Ravelli, S. Protti, A. Albini and M. Fagnoni, *Chem.-Eur. J.*, 2014, **20**, 17572–17578.
- 18 Z.-Y. Tang and Q.-S. Hu, *J. Am. Chem. Soc.*, 2004, **126**, 3058–3059.
- 19 B. Alonso, D. Massiot, F. Babonneau, G. Brusatin, G. Della Giustina, P. Innocenzi and T. Kidchob, *Chem. Mater.*, 2005, **17**, 3172–3180.
- 20 A significant amount of formate ion, up to 2 mg L⁻¹ was observed, probably due to the degradation of G8Ge2.
- 21 G. Della Giustina, G. Brusatin, M. Guglielmi and F. Romanato, *Mater. Sci. Eng., C*, 2007, **27**, 1382–1385.
- 22 J. L. Stratenus and E. Havinga, *Recl. Trav. Chim. Pays-Bas*, 1966, **85**, 434–436.
- 23 C. Raviola, V. Canevari, S. Protti, A. Albini and M. Fagnoni, *Green Chem.*, 2013, **15**, 2704–2708.
- 24 H. Qrareya, S. Protti and M. Fagnoni, *J. Org. Chem.*, 2014, **79**, 11527–11533.
- 25 C. Coenjarts, F. Ortica, J. Cameron, G. Pohlers, A. Zampini, D. Desilets, H. Liu and J. C. Scaiano, *Chem. Mater.*, 2001, **13**, 2305–2312.
- 26 L. Johnstonn, N. Mathivan, F. Negri and W. Siebrand, *Can. J. Chem.*, 1993, **71**, 1655–1662; D. Shukla, N. P. Schepp, N. Mathivan and L. J. Johnston, *Can. J. Chem.*, 1997, **75**, 1820–1829.
- 27 See for example: Y. Kageyama, R. Ohshima, K. Sakurama, Y. Fujiwara, Y. Tanimoto, Y. Yamada and S. Aoki, *Chem. Pharm. Bull.*, 2009, **57**, 1257–1266; I. F. Molokov, Y. P. Tsentalovich, A. V. Yurkovskaya and R. Z. Sagdeev, *J. Photochem. Photobiol., A*, 1997, **110**, 159–165; A. K. Zarkadis, V. Georgakilas, G. P. Perdikomatis, A. Trifonov, G. G. Gurzadyan, S. Skoulika and M. G. Siskosa, *Photochem. Photobiol. Sci.*, 2005, **4**, 469–480.
- 28 M. Takezaki, N. Hirota and M. Terazima, *J. Phys. Chem. A*, 1997, **101**, 3443–3448.
- 29 See for instance G. M. Coppinger and E. R. Bell, *J. Phys. Chem.*, 1966, **70**, 3479–3489; M. M. Miranda and F. Galindo, in *Photochemistry of Organic Molecules in Isotropic and Anisotropic Media*, ed. V. Ramamurthy and K. S. Schanze, Marcel Dekker Inc., New York-Basel, 2003.
- 30 (a) M. Gohdo, T. Takamasu and M. Wakasa, *Phys. Chem. Chem. Phys.*, 2011, **13**, 755–761; (b) M. C. Jiménez,



- M. A. Miranda, J. C. Scaiano and R. Tormosa, *Chem. Commun.*, 1997, 1487–1488; (c) C. E. Kalmus and D. M. Hercules, *J. Am. Chem. Soc.*, 1974, **96**, 449–456.
- 31 C. X. Xue, R. S. Zhang, H. X. Liu, X. J. Yao, M. C. Liu, Z. D. Hu and B. T. Fan, *J. Chem. Inf. Comput. Sci.*, 2004, **44**, 669–677.
- 32 L. Brigo, E. Zanchetta, G. Della Giustina and G. Brusatin, *Proc. SPIE*, 2014, 9161.
- 33 R. H. Munday, J. R. Martinelli and S. L. Buchwald, *J. Am. Chem. Soc.*, 2008, **130**, 2754–2755.
- 34 J.-i. Kuroda, K. Inamoto, K. Hiroya and T. Doi, *Eur. J. Org. Chem.*, 2009, 2251–2261.
- 35 J. H. Choi, B. C. Lee, H. W. Lee and I. Lee, *J. Org. Chem.*, 2002, **67**, 1277–1281.
- 36 H.-D. Choi, P.-J. Seo and B.-W. Son, *Arch. Pharmacol. Res.*, 2002, **25**, 786–789.

